CUES:
An Introduction to Coronal Velocity Distributions and the Modeling of UVCS/SOHO Emission Lines

Steven R. Cranmer
Smithsonian Astrophysical Observatory, 60 Garden Street, Cambridge, MA 02138
Email: scranmer@cfa.harvard.edu
WWW: http://cfa-www.harvard.edu/∼scranmer/

VERSION 1.1: January 29, 1998

1. Introduction

This set of notes contains a basic outline of the most relevant aspects of particle velocity distributions in the solar corona, and how they have an impact on the spectral lines that are observed by UVCS/SOHO. It also provides documentation for the CUES numerical code which computes model coronal lines from input velocity distribution parameters. These notes were originally written for undergraduate students who had no prior experience in solar physics or radiative transfer, so I have attempted to keep the discussion at an introductory level. Please give me feedback if I have aimed too high or too low in various areas, however.

With the information in this document, it will hopefully be possible for the reader to begin to compare actual UVCS data with empirical models of the spectral lines, and to adjust the parameters of the velocity distributions until there is agreement between the data and the models. However, the CUES code to be described below is only intended to be a basic "template" for further modeling efforts, and not a finalized production-code for generating research-quality results.

2. Particle Velocity Distributions

The information in this Section can be found in many thermodynamics or statistical mechanics textbooks; see, for example, Sears & Salinger [1975], Kittel & Kroemer [1980], or Morse [1964]. Even more general texts such as Tipler's [1978] *Modern Physics* contain a decent introduction to the kinetic theory of particle distributions. (See Reference Section on page 19 for a complete bibliography.)

Gases and plasmas are comprised of very large numbers of particles. It would be a very unwieldy task to follow the motion of each particle, so in order to understand the physics in these very complicated systems, we assume that at each point in space there is a *probability distribution* of many different velocities. (This has nothing to do with quantum mechanics, by the way – it is just a convenient way of treating large numbers of particles as a kind of "continuum" of unresolved overlapping states.) These distributions tell us the chances of finding particles that are moving at any arbitrary velocity $\mathbf{v}$.

Also, if one integrates these velocity distribution functions over all possible velocities, one obtains useful information about the "bulk" fluid properties of the gas or plasma: its local density, its overall drift velocity (or, for the solar wind, *outflow* velocity), and its thermal properties, such as temperature.

The simplest possible velocity distribution is that for the case of every single particle moving at the same velocity (speed and direction) $\mathbf{v}_0$. Of course, this never occurs in nature, but it nicely illustrates how these distributions work. This distribution would be proportional to a Dirac delta function:

$$f(\mathbf{v}) = n\, \delta(\mathbf{v} - \mathbf{v}_0) \tag{1}$$

where n is the local *number density* of particles, or the number of particles per unit volume (usually expressed in units of cm^{-3}). When integrating over all velocities, the result is simply n. This result holds for all properly-normalized distributions, and can be used as a general definition of the number density:

$$n \equiv \int f(\mathbf{v})\, d^3\mathbf{v} \ . \tag{2}$$

The most common velocity distribution in terrestrial environments is is the Maxwell-Boltzmann distribution, which is given by a Gaussian function of the velocity magnitude $v = |\mathbf{v}|$,

$$f(v) = \frac{n}{\pi^{3/2} w^3}\, e^{-v^2/w^2} \tag{3}$$

where $v^2 = v_x^2 + v_y^2 + v_z^2$. The so-called *thermal speed* is denoted by w, and this is the most-probable speed of particles in the distribution. In this distribution, however, there are particles with all possible speeds, from 0 to $+\infty$. The thermal speed w is related to the temperature of the gas or plasma by

$$w = \sqrt{\frac{2kT}{m}} \ , \tag{4}$$

where k is Boltzmann's constant and m is the mass of a particle. Thus it is easy to see that kT represents a most-probable kinetic energy of the particles $(mw^2/2)$, and it is of the same order as the *average* kinetic energy in a gas $(3kT/2)$ as derived in thermodynamics. The factor of $\pi^{3/2}w^3$ in the denominator of equation (3) makes sure that the distribution is normalized to n when integrating over all velocities.

(Exercise: Prove that w is the most probable speed by finding the maximum of the *speed distribution* $g(v) = 4\pi v^2 f(v)$. Why are the velocity and speed distributions different?)

Another useful quantity to extract from f is the mean drift velocity of the particles, or the *outflow velocity* for the solar wind. This is a vector quantity, defined by

$$\mathbf{u} \equiv \frac{1}{n} \int f(\mathbf{v})\, \mathbf{v}\, d^3\mathbf{v} \ . \tag{5}$$

For the simple delta-function distribution in equation (1), $\mathbf{u} = \mathbf{v}_0$, as one would expect. For the Maxwell-Boltzmann distribution in equation (3), $\mathbf{u}$ is zero! This makes sense physically, because a Maxwellian distribution is the *lowest energy* state of a gas; any bulk motion of the particles would result in a larger kinetic energy of the system.

However, here on Earth we do experience gases that are in bulk motion; the air on a windy day is a good example. These are best modeled by so-called "drifting Maxwellian distributions:"

$$f(\mathbf{v}) = \frac{n}{\pi^{3/2}w^3} \exp\left[-\frac{|\mathbf{v}-\mathbf{u}|^2}{w^2}\right] \ , \tag{6}$$

where $\mathbf{u}$ satisfies its definition above.

(Exercise: Prove that equation (5) is satisfied for a drifting Maxwellian, with $\mathbf{u} = u\,\hat{\mathbf{e}}_z$ and $d^3\mathbf{v} = dv_x\, dv_y\, dv_z$. The integrals in each direction span the entire "velocity space" from $-\infty$ to $+\infty$.)

In the solar wind, there are processes which make the temperature *anisotropic,* or different when viewed from different directions. From a thermodynamic point of view, this is very out of the ordinary, because this implies there must be processes in the solar wind that keep the system *away* from a single-temperature "thermal equilibrium." The most general way to express this situation is by splitting up the terms in the Maxwellian exponential into each Cartesian direction:

$$f(\mathbf{v}) = \frac{n}{\pi^{3/2}w_x w_y w_z} \exp\left[-\left(\frac{v_x-u_x}{w_x}\right)^2 - \left(\frac{v_y-u_y}{w_y}\right)^2 - \left(\frac{v_z-u_z}{w_z}\right)^2\right] \ . \tag{7}$$

Since this distribution is no longer strictly "thermal," let us call w_x, w_y, and w_z the *microscopic* most-probable speeds in the three directions, instead of thermal speeds. These can be used to compute the temperatures in the three directions, using equation (4), but it is debatable whether one can still validly use the word "temperature" in this case! The term sometimes used is *kinetic temperature,* which refers to the fact that they are only "temperature-like" numbers which correspond to the non-thermal microscopic motions of the particles in different directions.

Finally, the above distribution can be slightly simplified for use in models of the solar wind. In the accelerating regions of the corona seen by UVCS/SOHO, the solar *magnetic field lines* are usually pointing away from the sun, and the only relevant directions are *parallel* and *perpendicular* to this field. Let us then transform the velocity-space coordinates from Cartesian to cylindrical polar, and let us also assume that the magnetic field lines are parallel to the z axis:

$$v_x = v_\perp \cos\psi \tag{8}$$

$$v_y = v_\perp \sin\psi \tag{9}$$

$$v_z = v_\parallel \tag{10}$$

Let us also assume that the x and y directions are completely equivalent, so they have the same microscopic most-parallel speeds, $w_x = w_y \equiv w_\perp$. In addition, we can also assume that the only bulk outflow is *along* the magnetic field, and thus $u_\perp = 0$. The above anisotropic distribution then becomes the so-called "bi-Maxwellian" distribution, which is what we use to model the solar corona seen by UVCS/SOHO:

$$f(\mathbf{v}) = \frac{n}{\pi^{3/2} w_\parallel w_\perp^2} \exp\left[-\left(\frac{v_\parallel - u_\parallel}{w_\parallel}\right)^2 - \left(\frac{v_\perp}{w_\perp}\right)^2 \right] \ . \tag{11}$$

Note that there is no dependence on the azimuthal velocity-space coordinate ψ anywhere in the distribution. This makes sense when considering that *individual* charged particles under the influence of a magnetic field make gyrating, helix motions around the field-lines, called Larmor orbits. If one averages over a time that is long compared to the orbital period (which is only about 0.001 seconds for ions in the solar corona!), there is an equal chance for particles to be at any value of the ψ coordinate in velocity space, and thus no overall dependence on ψ.

IMPORTANT NOTE: The solar corona is made up of many different kinds of particles: both different chemical elements *and* different ionization stages of the same element. Because the most of the corona is so tenuous, and collisions between particles are so infrequent, *each* type of particle can have its own unique velocity distribution. Thus, each atom and ion (and also the free electrons) has its own independent values of $\{n, u_\parallel, w_\parallel, w_\perp\}$. Our eventual goal is to determine these parameters for various particles that we observe in ultraviolet spectra using UVCS.

3. Formation of Spectral Lines

In this Section I will give a broad (but not too deep) overview of how the velocity distributions affect the emergent radiation from the solar corona. More information can be found in books on stellar atmospheres (for example, Novotny [1973], if the reader is unfamiliar with the subject; also Mihalas [1978] and Collins [1989], for more details), or review papers on the corona (for example, Withbroe et al. [1982]). Also, I have produced several online notes which contain many of the details behind these derivations; they are on the WWW, accessible from:

`http://cfa-www.harvard.edu/~scranmer/cranmer_solar.html`

and the two most relevant files (in postscript form, ready to print) are at:

`http://cfa-www.harvard.edu/~scranmer/Preprints/uvcs_cues.ps`
`http://cfa-www.harvard.edu/~scranmer/Preprints/uvcs_pb.ps`

The adventurous reader, eager to learn more about how various strange and exotic *non-Maxwellian* distributions affect the spectral lines, can download my preprint on this subject, at:

`http://cfa-www.harvard.edu/~scranmer/cranmer_preprint.html`

We measure photons coming from the solar corona as counts on a detector, and these are translated into a *specific intensity* I_λ of the radiation. The specific intensity is the amount of energy per unit time, per unit wavelength, that passes through a unit solid angle in a certain direction. Thus, the units of specific intensity are often written (in cgs units) as

$$[I_\lambda] = \frac{\text{erg}}{\text{s cm sterad cm}^2} \quad , \tag{12}$$

but for convenience we express the wavelength units in Ångstroms and divide by the energy $h\nu$ of a single photon, to obtain the standard units:

$$[I_\lambda] = \frac{\text{photons}}{\text{s Å sterad cm}^2} \quad . \tag{13}$$

Because of the "per unit solid angle" in the definition of I_λ, the intensity is independent of the distance from the source of radiation. This is unlike the *flux* of radiation, which drops off, for example, as the inverse square of the distance from a spherical or point source (see, for example, Novotny [1973] for more details).

The electromagnetic radiation emitted by the tenuous solar corona arises mainly within narrow bands of wavelength, in spectral *emission lines.* This is in drastic contrast to the radiation emitted by the solar photosphere, which is mainly spread out in a broad-band continuum, with spectral lines being only a relatively minor perturbation. In the *ultraviolet* wavelengths observed by UVCS/SOHO in the corona, there is virtually no continuum at all.

The photons emitted by the corona in spectral lines arise from two primary microscopic phenomena:

1. *Scattering of photons from the bright solar disk.* Incoming photons from the photosphere and chromosphere can impact bound atoms and ions in the corona, causing their electrons to jump into excited states. A fraction of a second later, these electrons "decay" back down to their ground level, and the atom re-emits a photon at the wavelength corresponding to the energy-difference between the two levels. Unlike the incoming photon, which came from a well-defined spatial source, the outgoing photon is emitted in a random direction. [1]

2. *Collisions between atoms and free electrons.* In the corona, the free electrons have temperatures similar to the temperatures of the other atoms and ions. Electrons are ∼1840 times lighter than any particle with a nucleus, so from equation (4) we know they are moving, on average, ∼43 time *faster.* These tiny "bullets" often ricochet off atoms, losing some of their kinetic energy in the process. Like in the scattering of photons, above, this new "input" of energy to the atom is used to temporarily raise up the energy-level of one or more of its bound electrons, and eventually this energy is re-emitted as a photon.

For a given pair of atomic energy levels, these two processes produce photons at a single "monochromatic" wavelength. (Heisenberg's Uncertainty Principle ensures that it is not *truly* monochromatic, but for our purposes all the terms in $[\Delta E\,\Delta t \sim \hbar]$ are negligibly small.)

However, these emitting atoms are not sitting still in the corona. As we have seen in Section 2, they are moving with a whole host of random velocities, specified by $f(\mathbf{v})$. The photons that we see, then, get *Doppler shifted* because they come from moving sources.

[1] Photons can also be scattered by *free electrons;* this is known in the relativistic limit as Compton scattering, and in the non-relativistic limit as Thomson scattering. The latter is the cause of a non-zero *polarization* of the observed coronal radiation, and is what the UVCS White Light Channel (WLC) measures to deduce the electron density n_e. These notes will not contain anything further about the WLC, but see, for example, Strachan et al. [1993], Guhathakurta & Holzer [1994], or my online notes (`uvcs_pb.ps`), about this important diagnostic.

This is what makes the spectral lines have a definite shape, and *not* look like simple delta functions at the atomic transition wavelength!

Thus, the goal of the "empirical modeling" process is to simulate the appearance of the specific intensity I_λ in these spectral lines – using known velocity distribution parameters. As we vary these parameters, the emerging intensity changes, and we can compare the synthetic lines to the observed lines, and thus deduce valuable information about the actual velocity distributions.

(You might be curious to also learn about space missions such as *Ulysses,* which have flown in the solar wind and gathered information about velocity distributions by *collecting particles.* However, none of these spacecraft have been hardy enough to fly so close to the sun as we observe with UVCS/SOHO. Our kind of remote-sensing observations currently provide the only information about this important region of the corona, where the solar wind is initially accelerated away from the sun.)

The corona is extremely tenuous and transparent, so each observation effectively collects information about the photons emitted along the entire *line-of-sight* (LOS); see Figure 1. The specific intensity is thus an integral over the LOS of a local *emissivity* j_λ of photons:

$$I_\lambda(\rho) \;=\; \int_{-\infty}^{+\infty} j_\lambda(\rho, x)\, dx \tag{14}$$

where x is the distance along the LOS, ρ is the sun-centered "projected radius" to which we point UVCS (i.e., the "impact parameter" in the plane of the sky), and $r = (x^2 + \rho^2)^{1/2}$ is the actual radius to each point in the wind. In the CUES code to be discussed below, we assume that the emissivity depends only on this radius, so $j_\lambda(\rho, x) = j_\lambda(r)$.

How does j_λ depend on the velocity distribution of the particles? First, j_λ depends linearly on the number density of atoms n; this makes sense because more particles produce more photons. (Only in very rare cases, such as coronal mass ejections [CMEs], does the corona become so dense and *opaque* that this simple relationship breaks down.)

For photons produced by **collisional excitation**, we can write the emissivity as

$$j_\lambda^{(\mathrm{coll})} \;=\; \frac{1}{4\pi} n_i\, n_e\, q_{12}(T_e)\, \phi(\lambda) \;\; , \tag{15}$$

where n_i is the number density of the bound atom or ion that was excited, n_e is the number density of free electrons (because more electrons produce more collisions, and thus more photons), and q_{12} is an effective *collision rate* per electron, which depends mainly on the electron temperature T_e. These rates have been computed from quantum-mechanical scattering theory, and are tabulated in the CUES program. The function $\phi(\lambda)$ is the so-called *line profile function*, which contains the details of the Doppler shifts due to the local velocity

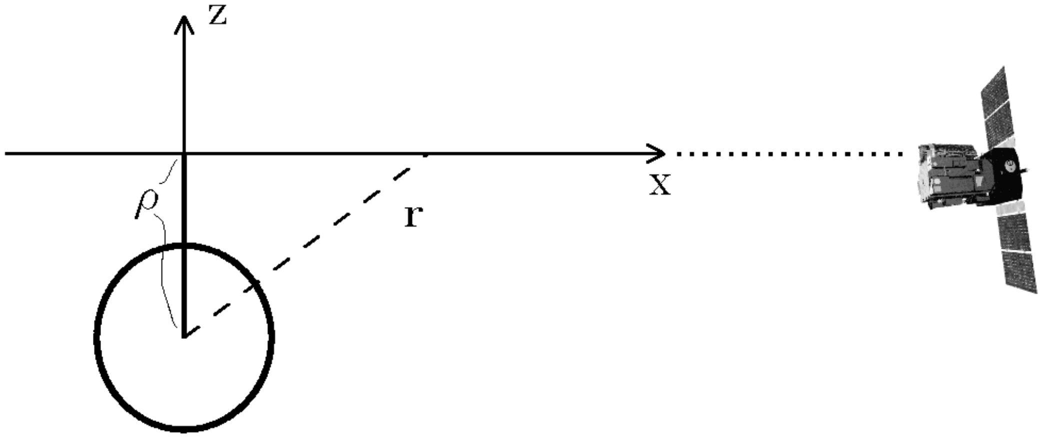

Fig. 1.— Line-of-sight (LOS) geometry in the solar wind. The observed intensity arises from contributions all along the x axis.

distribution. One can express it in general by

$$\phi(\lambda) \;=\; \frac{1}{n} \int f(\mathbf{v})\, \delta \left[\frac{\lambda_0}{c} v_{\rm LOS} - (\lambda - \lambda_0) \right] d^3\mathbf{v} \;\;, \tag{16}$$

where λ_0 is the line-center "rest wavelength" of the transition and $v_{\rm LOS}$ is the projected component of $\mathbf{v}$ along the LOS. The delta function above performs the Doppler "transformation" from velocity to wavelength units.

For the drifting bi-Maxwellian defined in equation (11), we find (for $v_{\rm LOS} = v_x$) that the profile is a Gaussian:

$$\phi(\lambda) \;=\; \frac{1}{\Delta\lambda \sqrt{\pi}} \exp \left[- \left(\frac{\lambda - \lambda_0}{\Delta\lambda} \right)^2 \right] \;\;, \tag{17}$$

where $\Delta\lambda = (\lambda_0 w_\perp / c)$. Of course, this strictly applies only at the point $x = 0$ (or $\rho = r$); see Figure 1. For all other points along the LOS, $v_{\rm LOS}$ is combination of v_x and v_z, and $\Delta\lambda$ contains a contribution from both $w_\perp$ and $w_\parallel$. But because the number densities n_i and n_e *decrease rapidly* with increasing radius, these extended regions along the LOS are not as important to the I_λ integral as the most central region around $x = 0$. (However, the CUES code computes $\phi(\lambda)$ correctly for all points.)

For photons produced by **scattering of solar-disk photons** (often called *resonance scattering* because the lines we observe are "resonance" lines between the lowest $n = 1$ and $n = 2$ atomic levels), the emissivity j_λ is more complicated to express. It now depends not only on the density of atoms, but also on the wavelength, direction, and intensity of all the *incoming* photons.

The emissivity of a scattering line can be represented by

$$j_\lambda^{\rm (scat)} \;=\; \frac{B_{12}}{4\pi}\, n_i \int_0^\infty d\lambda' \oint \frac{d\Omega'}{4\pi}\, R(\lambda', \lambda, \hat{\mathbf{n}}', \hat{\mathbf{n}})\, \tilde{I}_{\lambda'}(\hat{\mathbf{n}}') \;\;, \tag{18}$$

where the integrals are over the incoming wavelength λ' and direction (unit vector $\hat{\mathbf{n}}'$ over solid angle Ω') of photons from the solar disk. The *outgoing* photon is also specified by a wavelength λ and a direction $\hat{\mathbf{n}} = \hat{\mathbf{e}}_x$ (see Figure 1), but the scattering process which transforms incoming to outgoing photons is specified by the (often complicated) "redistribution function" R, which depends on $f(\mathbf{v})$. Also, j_λ depends on the incident intensity profile $\tilde{I}_{\lambda'}$ (which is measured by observing the line of interest on the solar disk), and on the atomic *absorption rate* B_{12}, which is computed from quantum mechanics (like q_{12}) and is tabulated within the CUES code for various spectral lines.

It is important to note that $j_\lambda^{\rm (scat)}$ depends on n_i just as $j_\lambda^{\rm (coll)}$ does, but there is only one density factor present in the scattering emissivity, while there are two (n_i and n_e) in the collisional emissivity. Because the number densities of "minority" atoms and ions are often expressed as *fractions* of the electron density n_e, the $j_\lambda^{(\rm scat)}$ and $j_\lambda^{(\rm coll)}$ emissivities are often referred to as being dependent on n_e and n_e^2, respectively (where each is multiplied by the fraction n_i/n_e, of course). Different spectral lines are formed by different relative combinations of scattering and collisional processes, so some lines "sample" the density over the LOS, others sample the square of the density, and others sample a linear combination of the two.

The derivation of the redistribution function R is outlined in detail in my online notes (`uvcs_cues.ps`), and here I intend to only present an approximate form which allows most of the important ideas of resonance scattering to be understood. For the simple case of right-angle scattering (i.e., at the point $x = 0$ along the LOS) of a photon that came from the center of the sun, and from a *very narrow* solar-disk line,[2] the scattering emissivity is approximately proportional to

$$j_\lambda^{(\rm scat)} \propto \frac{B_{12}}{4\pi} n_i \tilde{I}_{\lambda_0} \exp\left[- \left(\frac{\lambda - \lambda_0}{\Delta\lambda} \right)^2 \right] \exp\left[- \left(\frac{u_\parallel}{w_\parallel} \right)^2 \right] \quad , \tag{19}$$

where $\Delta\lambda = (\lambda_0 w_\perp / c)$, and $\tilde{I}_{\lambda_0}$ is the specific intensity at the center of the incoming solar-disk spectral line. Notice the line shape *in wavelength* is Gaussian, as in the case of collisional excitation, but now there is also a dependence on the parallel outflow speed $u_\parallel$ and the parallel microscopic speed $w_\parallel$. This effect is called **Doppler dimming,** because the existence of an outflow velocity (*not* necessarily along the LOS!) diminishes the emissivity, and thus also the integrated intensity I_λ.

One can understand Doppler dimming in a heuristic way by imagining how the existence of an outflow velocity $u_\parallel$ affects the local line profile function $\phi(\lambda)$ *in the parallel direction* – i.e., for $v_{\rm LOS} = v_z$ in equation (16). (We cannot observe the profile in this direction, but the photons streaming from the solar disk can!) The function $\phi(\lambda)$ gets redshifted from line-center by the quantity $(\lambda_0 u_\parallel / c)$. However, the *source* of incoming photons $\tilde{I}_\lambda$ is still centered on λ_0. The greater the value of $u_\parallel$, the less overlap there is between the incoming profile and the local coronal profile – and thus fewer photons can be scattered, leading to an overall dimming of the emissivity. [3]

---

[2] Most lines which arise on the solar disk are narrow in wavelength compared to their counterparts formed *locally* in the corona. This is why the UVCS instrumental "stray light" from the disk often looks like a narrow peak on top of the broad coronal profile.

[3] In addition to dimming, sometimes the scattering can be *enhanced* by the presence of other, nearby solar-disk lines. This "Doppler pumping" occurs when the local coronal profile gets redshifted away from its own solar-disk line, and begins to come under the influence of additional sources of photons (i.e., other lines!). The O VI λ1037 line exhibits this effect; see Noci et al. [1987] for a detailed description of how this can be used as a *diagnostic* for the outflow speed.

IMPORTANT NOTE: The *parallel* microscopic motions of particles tend to most strongly affect the Doppler dimming of the entire line, while the *perpendicular* microscopic motions tend to most strongly affect the shape of the line. One can start out by treating these two "diagnostics" independently, but eventually both must be combined into a single model of the velocity distribution which produces both effects together.

Most of the numerical complexity of the CUES code is devoted toward computing the redistribution function R (and its integral in equation [18]) in all its gory detail, for arbitrary points along the LOS and arbitrary photon directions and wavelengths. The resulting profiles and Doppler dimming may not behave in the simple way expressed in equation (19), but the numerical results are often not too different from this approximate form. One difference to keep in mind is that the line widths due to collisional and scattering processes may not be the same, despite the approximate forms presented above.

4. Running the CUES Code

The Fortran program CUES (which stands for **C**oronal **U**ltraviolet **E**mission **S**ynthesis) is a slightly-simplified version of a program which is currently being used to produce empirical models of UVCS/SOHO data in our ongoing research. The simplifications in the code basically mean that the user does not have the full freedom to specify the *three-dimensional* distribution of density, outflow velocity, and the microscopic speeds in the model corona. The parameters that can be chosen still allow much of the physics in the corona to be explored and modeled, however. Researchers using this code have the freedom to edit it appropriately to conform to their individual situations, but we urge users to explore what the present version of the code can do before making modifications.

What follows is a listing of the files in the primary CUES directory.

`cues.f`	The Fortran source code for the main program and all subroutines.
`cues.x`	The executable program to run, compiled on a Sun Solaris SPARCstation 4.
`cues_inc.f`	Source code that is included at the beginning of each subroutine, containing variable declarations, common blocks, etc.
`doc_cues.ps`	The postscript version of these "documentation" notes you are reading.

`sample_lya.in`	An example input file that computes an H I Lyman alpha line profile. [4]
`sample_lya.out`	The output that should be generated by the input file of the same name.
`sample_ovi1032.in`	An example input file that computes an O VI λ1032 line profile.
`sample_ovi1032.out`	The output that should be generated by the input file of the same name.
`sample_ovi1037.in`	An example input file that computes an O VI λ1037 line profile.
`sample_ovi1037.out`	The output that should be generated by the input file of the same name.

One runs the program by first creating an input file, which contains all the adjustable parameters that can be varied in the code. At first, it will probably be useful to start by making personal copies of the `sample*.in` files, and experiment by changing a few of the parameters in those files. Assuming the input file is named `myinput.in`, and the user wants to put the output into a file named `myoutput.out`, the code is executed by typing the following command on a UNIX workstation:

```
cues.x < myinput.in > myoutput.out &
```

This assumes the current directory contains the executable file `cues.x`. Also, the ampersand (`&`) at the end runs the code as a background process, so that, depending on the speed of the computer on which the code is run, one can monitor the output file as it is created. (On some machines, though, the code will run in just a few seconds, and the ampersand is not needed.)

All the parameters to vary are in the **input file**, so it is worthwhile to go over each item in this file in detail. Figure 2 shows the example input file `sample_lya.in`. The input file must always contain the same number of lines (10), and the order of the items cannot be changed. The comments to the right of the exclamation points are there to help the user remember which variables are on which lines.

[4] The roman-numeral spectroscopic notation denotes the atom or ion which generates the spectral line. The roman numeral is 1 plus the number of excess positive charges in the atom or ion. Thus, H I denotes H^0 (a neutral hydrogen atom), and O VI denotes O^{5+} (an oxygen ion with 5 electrons removed). The central wavelength of the line is denoted by λ followed by the wavelength in Ångstroms, or by a unique name for a well-known transition, such as Lyman α.

```
          1      ! Type of diagnostic to model
       2.00      ! Observing radius (impact parameter), in solar radii
         15      ! LAMBDA: number of wavelength points to compute
    1213.20      ! LAMBDA: wavelength lower limit (in Angstroms)
    1218.20      ! LAMBDA: wavelength upper limit (in Angstroms)
       1.00      ! Electron Density multiplier (N)
 1.5000e+06      ! Electron Temperature (in Kelvin)
       1.00      ! Ion outflow velocity multiplier (U)
     200.00      ! Ion parallel      microscopic speed, w_para (in km/s)
     250.00      ! Ion perpendicular microscopic speed, w_perp (in km/s)
```

Fig. 2.— Example input file to CUES (sample_lya.in).

The 10 input parameters are as follows:

- **Diagnostic:** This is an integer number that specifies the type of diagnostic to compute. The full list of choices is given in the first few lines of the Fortran source file `cues.f`, but the a few of the most common diagnostics are:

1	H I λ1215.67 (Hydrogen Lyman alpha)
3	H I λ1025.72 (Hydrogen Lyman beta)
10	O VI λ1031.93 (Oxygen 1032 Å)
11	O VI λ1037.62 (Oxygen 1037 Å)
0	White Light polarization brightness (pB)

- **Radius:** This number is $(\rho/R_\odot)$, or the minimum distance of the LOS from the center of the sun, in units of the solar radius $R_\odot$. This is the simulated "mirror position," or pointing, of the UVCS telescope.

- **Wavelength:** The next three lines contain (1) the number of wavelengths to compute, (2) the minimum wavelength in Ångstroms, and (3) the maximum wavelength in Ångstroms. The intermediary wavelengths will be computed on an evenly-spaced grid.

- **Electron Density:** This dimensionless number is N, the multiplier to be applied to the assumed radial dependence of electron density n_e (see below).

- **Electron Temperature:** This is the actual electron temperature T_e (in Kelvin) that is assumed for all points along the LOS.

- **Outflow Velocity:** This dimensionless number is U, the multiplier to be applied to the assumed radial dependence of outflow velocity $u_\parallel$ of the ion under consideration (see below).

- **Bi-Maxwellian Microscopic Speeds:** These last two lines of the input file contain $w_\parallel$ and $w_\perp$ for the ion under consideration, respectively. These values are assumed constant along the LOS, and they are input in units of km s^{-1}.

As mentioned above, the primary limitation to the CUES code is that there is not full control over the full 3D variation of the various velocity distribution parameters. The electron temperature T_e and the ion microscopic speeds ($w_\parallel$ and $w_\perp$) are assumed to be *constant* along the LOS, mainly because they have not been observed to vary extremely sharply with radius. The electron density n_e and the ion outflow velocity $u_\parallel$, however, do vary quickly as functions of radius. Thus, it is important to include these variations as the code integrates numerically over different points along the LOS. We have decided to use standardized radial "laws" for these two parameters, but still allow the user to have some control by multiplying these laws by arbitrary constants (N and U).

The electron number density in the corona is given by a constant number N multiplied by the radial variation of n_e given by Guhathakurta & Holzer [1994] for polar coronal-hole regions around the minimum of the solar cycle. Thus, we use:

$$n_e(r) \;=\; N \left[1.4 \times 10^6 \left(\frac{R_\odot}{r} \right)^{2.8} + 8.0 \times 10^7 \left(\frac{R_\odot}{r} \right)^{8.45} + 8.1 \times 10^7 \left(\frac{R_\odot}{r} \right)^{16.87} \right] \; \mathrm{cm}^{-3} \quad . \tag{20}$$

When modeling observations over the north and south coronal poles (i.e., in the dark regions known as *coronal holes*), one can safely assume $N = 1$. When modeling the bright *streamers* around the Sun's equatorial regions, the density is significantly higher than over the poles. A good starting estimate is to try $N = 6$, but this is not always valid; observations have found values of N in streamers between 3 and 10.

(The standard practice in modeling UVCS/SOHO data is to use electron density values gathered from other observations, for example, the White Light polarization brightness, or pB, data from the UVCS WLC instrument, or from the LASCO coronagraph on SOHO, or from ground-based coronagraphs. If one already knows n_e at a specific radius r, it is then possible to solve for N, which then may be applied to all other radii.)

The outflow velocity is given by assuming *mass flux conservation* for radial flow in the steady-state solar wind. The conserved flux of number-density in a "flow tube" of cross-sectional area A is defined by

$$(n_e \, u_\parallel \, A) \;=\; \text{constant} \quad , \tag{21}$$

and for radial flow in spherical symmetry, A is proportional to r^2. If we use data gathered by spacecraft (at a radius of 1 AU) to set the constant, we can solve for the outflow velocity at other radii, and multiply it by an arbitrary factor U that the user can control:

$$u_\parallel(r) \;=\; U \left[\frac{(n_e \, u_\parallel \, r^2)_{1\,\mathrm{AU}}}{n_e \, r^2} \right] \tag{22}$$

where the quantities in the numerator are evaluated at a radius of 1 AU, which has been probed consistently with spacecraft. At $r_{1\,\mathrm{AU}} = 215 \, R_\odot = 1.496 \times 10^{13}$ cm, the measured electron number-density flux for the fast solar wind is $n_e u \approx 2.5 \times 10^8 \, \mathrm{cm}^{-2} \mathrm{s}^{-1}$. When modeling observations over polar coronal holes, U is typically about 1 or 1.5, but can be a bit larger for lines formed by heavier ions (like O VI). When modeling observations in streamers, the outflow velocities are typically smaller, and even *no outflow* (i.e., $U = 0$) may best reproduce the data in some cases.

Notice that one may use different values of N and U for different observation radii ρ. This is not totally self-consistent, because for given values of N and U the code actually specifies the density and outflow velocity for all $r \geq \rho$. However, points along the *extended* LOS (i.e., for $r \gg \rho$) do not contribute significantly to the intensity, and it often does not matter what the code assumes for these points. Thus, one can leave open the possibility that the radial forms for n_e and $u_\parallel$ are not valid, and one can attempt to correct them by varying N and U as functions of ρ. One can also vary T_e, $w_\parallel$, and $w_\perp$ as functions of ρ for the same reasons.

The CUES code takes the above-defined input parameters, and numerically integrates over the incident intensity λ', the incident photon solid angle Ω', and over the LOS variable x. The output intensity is the sum of the collisional and scattering components. At the end, the code performs an additional integration over the wavelength of the outgoing photons, in order to evaluate the total line-integrated intensity $I_{\rm tot}$:

$$I_{\rm tot} \, = \, \int_{-\infty}^{+\infty} I_\lambda \, d\lambda \ \ . \tag{23}$$

Computationally, of course, the limits of this integrand are set by the user's choice for lower and upper limits on the wavelength grid. (If these limits are too narrow, resulting in some of the line being cut off and not included in the integral, the code will produce a warning.)

The integrated intensity $I_{\rm tot}$ is especially useful for examining the effects of Doppler dimming or Doppler pumping. As you may learn, not all UVCS/SOHO observations provide an accurate line profile; some only yield a reliable value for the total intensity. Even more reliable, in some cases, is the *ratio* of total intensities between pairs of similar lines, such as the O VI 1032 and 1037 doublet. This ratio is a convenient quantity to aid in deducing the outflow velocity $u_\parallel$.

Figure 3 displays the **output file** generated by the CUES program for the input data from Figure 2. On a Sun Solaris SPARCstation 4, it took about one minute to run the code for the 15 wavelength points computed.[5]

The process of varying the input parameters to find a valid model of the observed corona is not simple or straightforward. Unfortunately, there are more variables than constraints from the data. The safest procedure is to settle on a value for N relatively early in the process, whether from white-light data or from assumptions about the type of structure to be modeled. Also, the electron temperature T_e does not vary by very much, and most observations are relatively insensitive to this parameter; anything outside the range between, say, 0.7 and 2.5 million Kelvins should be questioned very critically.

---

[5] Occasionally when the code is run, the error message `Inexact; Underflow` will be output to the screen (i.e., to the "standard error" device). This message can be disregarded; it only means that the code attempted to take, say, the exponential of a very large negative number. The result was a number so small that it caused an "underflow," and it was replaced with zero, as it should have been.

```
 CUES:  Diagnostic = H I Lyman alpha

rho / R_sun    =  2.0000000         w_para  =   2.0000000E+02  km / s
N multiplier   =  1.0000000         w_perp  =   2.5000000E+02  km / s
U multiplier   =  1.0000000     T_electron  =   1.5000000E+06     K

       WAVELENGTH                INTENSITY
      (Angstroms)     (photons s-1 cm-2 sr-2, Angstrom-1)

     1.2132000E+03             3.6026548E+06
     1.2135571E+03             2.0028967E+07
     1.2139143E+03             8.7130693E+07
     1.2142714E+03             2.9640001E+08
     1.2146286E+03             7.8553319E+08
     1.2149857E+03             1.6056323E+09
     1.2153429E+03             2.4821471E+09
     1.2157000E+03             2.8305730E+09
     1.2160571E+03             2.3555673E+09
     1.2164143E+03             1.4538099E+09
     1.2167714E+03             6.8221470E+08
     1.2171286E+03             2.4825884E+08
     1.2174857E+03             7.0707788E+07
     1.2178429E+03             1.5823206E+07
     1.2182000E+03             2.7855671E+06

 Number of wavelength points =   15
 TOTAL Integrated Intensity  =  4.6215054E+09   (photons s-1 cm-2 sr-1)
```

Fig. 3.— Example output file from CUES (`sample_lya.out`), corresponding to the input parameters listed in Figure 2.

Thus, there are three primary parameters to vary (U, $w_\parallel$, and $w_\perp$), and two primary line-characteristics to model (total intensity $I_{\rm tot}$ and line width $\Delta\lambda$). In older papers, one simply used equation (4) to solve for $w_\parallel$, using the electron temperature as a proxy for the parallel kinetic temperature of the atom or ion. However, recent UVCS results have shown that the velocity distribution parameters for electrons, atoms, and ions are often very different from one another, and it is dangerous to assume that temperatures are the same for different species. (Possibly the only location where all temperatures are equal is very "deep" in streamers, i.e. at radii $r < 2$–$3\,R_\odot$; see Kohl et al. [1997]. Here the densities are so large that there are sufficient inter-particle collisions to maintain a true thermal equilibrium.)

In our empirical model work, we have assumed lower and upper limits on $w_\parallel$, and then varied the other two parameters for each case until there was detailed agreement between the modeled and observed line profiles (see Kohl et al. [1998] and Cranmer et al. [1998]). We thus obtained lower and upper limits on $u_\parallel$ and $w_\perp$.

If users of the CUES code have any questions or problems, please do not hesitate to contact me (`scranmer@cfa.harvard.edu`) or any other UVCS/SOHO team member.

REFERENCES

Arfken, G. B., & Weber, H. J. 1995, Mathematical Methods for Physicists, 4th ed. (San Diego: Academic Press)

Beckers, J. M., & Chipman, E. 1974, Sol. Phys., 34, 151

Chandrasekhar, S. 1960, Radiative Transfer (New York: Dover)

Collins, II, G. W. 1989, The Fundamentals of Stellar Astrophysics (New York: Freeman)

Cram, L. E., & Vardavas, I. M. 1978, Sol. Phys., 57, 27

Cranmer, S. R., et al. 1998, in preparation

Dreicer, H. 1959, Phys. Rev., 115, 238

Guhathakurta, M., & Holzer, T. E. 1994, ApJ, 426, 782

House, L. L. 1970, J. Quant. Spectrosc. Radiat. Transfer, 10, 909

Hummer, D. 1962, MNRAS, 125, 21

Hundhausen, A. J. 1972, Coronal Expansion and Solar Wind (Berlin: Springer-Verlag)

Hyder, C. L., & Lites, B. W. 1970, Sol. Phys., 14, 147

Kittel, C., & Kroemer, H. 1980, Thermal Physics, 2nd ed. (New York: W. H. Freeman)

Kohl, J. L., Esser, R., Gardner, L. D., Habbal, S., Daigneau, P. S., Dennis, E. F., Nystrom, G. U., Panasyuk, A., Raymond, J. C., Smith, P. L., Strachan, L., van Ballegooijen, A. A., Noci, G., Fineschi, S., Romoli, M., Ciaravella, A., Modigliani, A., Huber, M. C. E., Antonucci, E., Benna, C., Giordano, S., Tondello, G., Nicolosi, P., Naletto, G., Pernechele, C., Spadaro, D., Poletto, G., Livi, S., von der Lühe, O., Geiss, J., Timothy, J. G., Gloeckler, G., Allegra, A., Basile, G., Brusa, R., Wood, B., Siegmund, O. H. W., Fowler, W., Fisher, R., & Jhabvala, M. 1995, Sol. Phys., 162, 313

Kohl, J. L., et al. 1997, Sol. Phys., 175, 613

Kohl, J. L., et al. 1998, ApJ, submitted

Kohl, J. L., Strachan, L., & Gardner, L. D. 1996, ApJ, 465, L141

Kohl, J. L., & Withbroe, G. L. 1982, ApJ, 256, 263

Kopp, R. A., & Holzer, T. E. 1976, Sol. Phys., 49, 43

Mihalas, D. 1978, Stellar Atmospheres, 2nd ed. (San Francisco: W. H. Freeman)

Mihalas, D., & Mihalas, B. W. 1984, Foundations of Radiation Hydrodynamics (Oxford: Oxford U. Press)

Morse, P. M. 1964, Thermal Physics (New York: W. A. Benjamin)

Noci, G., Kohl, J. L., & Withbroe, G. L. 1987, ApJ, 315, 706

Novotny, E. 1973, Introduction to Stellar Atmospheres and Interiors (New York: Oxford University Press)

Olsen, E. L., Leer, E., & Holzer, T. E. 1994, ApJ, 420, 913

Parker, E. N. 1958, ApJ, 128, 664

Parker, E. N. 1963, Interplanetary Dynamical Processes (New York: Interscience Publishers)

Parker, E. N. 1966, ApJ, 143, 32

Pneuman, G. W., & Kopp, R. A. 1971, Sol. Phys., 18, 258

Press, W. H., Flannery, B. P., Teukolsky, S. A., & Vetterling, W. T. 1989, Numerical Recipes: The Art of Scientific Computing (Cambridge: Cambridge U. Press)

Raymond, J. C., et al. 1997, Sol. Phys., 175, 645

Sears, F. W., & Salinger, G. L. 1975, Thermodynamics, Kinetic Theory, and Statistical Thermodynamics, 3rd ed. (Reading, Massachusetts: Addison-Wesley)

Strachan, L., Kohl, J. L., Weiser, H., Withbroe, G. L., & Munro, R. H. 1993, ApJ, 412, 410

Tipler, P. A. 1978, Modern Physics (New York: Worth Publishers)

Verner, D. A., Verner, E. M., & Ferland, G. J. 1996, Atomic Data Nucl. Data Tables, 64, 1

Withbroe, G. L. 1970, Sol. Phys., 11, 42

Withbroe, G. L., Kohl, J. L., Weiser, H., & Munro, R. H. 1982, Space Sci. Rev., 33, 17
